

Structural determination of the S-passivated InP(100)-(1×1) surface by dynamical low-energy electron-diffraction analysis

O. L. Warren, G. W. Anderson, M. C. Hanf, K. Griffiths, and P. R. Norton

Interface Science Western and the Department of Chemistry, The University of Western Ontario, London, Ontario, Canada N6A 5B7

(Received 21 April 1995)

We have determined the optimum geometry of the S-passivated InP(100)-(1×1) surface by dynamical low-energy electron-diffraction analysis. S atoms bond to In by occupying the bridge site that continues the zinc-blende stacking sequence of the substrate. Other potential high-symmetry adsorption sites (atop, antibrige, and hollow) can be clearly ruled out. The overlayer-substrate interlayer spacing is found to be 1.445 ± 0.033 Å, and the topmost substrate interlayer spacing is found to be 1.465 ± 0.035 Å. Both values are close to the bulk interlayer spacing of 1.468 Å. We also have investigated the S coverage within the framework of the average *t*-matrix approximation, and our results favor a full monolayer. However, the coverage could be as low as 0.77 monolayer when the uncertainty is taken into account. The optimum geometry of the S-passivated surface is consistent with sp^3 -hybridized S and In forming predominantly covalent bonds, which has important implications with regard to the passivation mechanism.

I. INTRODUCTION

III-V compound semiconductors are recognized primarily for their potential applications in high-speed electronic and long-wavelength optical circuitry.¹ However, the high surface state density and the high surface recombination velocity of these materials have hampered the development of III-V devices.¹ Consequently, there is considerable interest in obtaining suitable techniques for treating the surface of the semiconductor, prior to subsequent processing, so that the surface states shift from the band gap and into the valence and conduction bands. This can be accomplished by chemically passivating the semiconductor surface.

In the case of InP(100), the surface is passivated effectively by reaction with inorganic sulfides.²⁻¹¹ Iyer, Chang, and Lile² have shown that the electrical properties of metal-insulator-semiconductor field-effect transistors fabricated from InP(100) can be greatly enhanced by pretreating the semiconductor surface in a heated aqueous solution of $(\text{NH}_4)_2\text{S}$, and subliming excess S in vacuum prior to growing SiO_2 . However, the amount of S at the surface spanned a wide range, which resulted in some variation in the measured electrical properties of the final product.³

Recently, Tao *et al.*⁵ advanced the process of pretreating InP(100) with aqueous $(\text{NH}_4)_2\text{S}$ by first heating the solution under intense illumination from white light, and then rinsing the sample with deionized water. Samples prepared in this manner exhibited a (1×1) low-energy electron-diffraction (LEED) pattern upon introduction into vacuum, in the absence of further treatment. Based on their x-ray photoelectron spectroscopy (XPS) results, Tao *et al.* concluded that the surface was passivated by approximately a full monolayer of S atoms that formed robust covalent bonds exclusively to In. As a further testament to the remarkable stability of the S-passivated surface, the samples still exhibited a (1×1) LEED pat-

tern after exposure to the atmosphere for several days. Later studies⁸⁻¹¹ have shown that illumination is not required to form a well-passivated surface, with XPS results again suggesting a S coverage of ~ 1 monolayer.⁸

In spite of the significant number of studies on S passivation of InP(100), a precise description of the resultant surface geometry has not yet emerged. Tao *et al.*⁵ proposed, without direct evidence, that the S atoms resided in bridge sites corresponding to P vacancies. Shortly thereafter, Lu *et al.*⁶ found support for this model in their E-polarization-dependent study of the x-ray-absorption near-edge structure (XANES) of the sulfur *K* edge, from which they estimated an In-S-In bond angle of 100° . Further work by Lu⁷ using x-ray photoelectron diffraction (XPD) indicated that this bond angle fell within the range of $100^\circ - 110^\circ$. While these studies provide information with regard to the resultant structure, along with some insight into the passivation mechanism, the surface geometry still remains ambiguous as only low-precision estimates for the In-S-In bond angle have been reported. In this paper, we present a complete and quantitative description of the optimum geometry of the S-passivated InP(100)-(1×1) surface, which we have determined by dynamical LEED analysis.

II. EXPERIMENTAL PROCEDURES

The experiments were carried out in a diffusion-pumped, μ -metal-shielded, ultrahigh-vacuum (UHV) chamber with a base pressure of less than 1×10^{-10} torr. The UHV chamber is equipped with a four-grid retarding field analyzer for LEED and a hemispherical electron energy analyzer for Auger electron spectroscopy (AES). The substrate was an undoped epilayer ($\sim 2 \mu\text{m}$ in thickness) grown on an InP(100) wafer by chemical beam epitaxy. The sample was prepared (as described previously^{10,11}) by first etching the substrate in 5% HF for 1 min, and then treating it for 20 min in an aqueous solution of

(NH₄)₂S, which was held at 340 K. After passivating the surface, the sample was thoroughly rinsed in running and static deionized water, dried with He, and introduced into the UHV chamber by a remote transfer arm housed in a turbopumped loadlock chamber. The pressure in the UHV chamber increased to $\sim 5 \times 10^{-10}$ torr after the sample transfer. In agreement with the work of Tao *et al.*,⁵ the observation of a (1×1) LEED pattern did not require further treatment. The sample cleanliness was verified by AES, which showed a trace of C contamination (O was not observed) in addition to S, In, and P. Annealing to 570 K for ~ 20 min (which has been shown not to destabilize the surface¹⁰) was found to remove the C contamination as well as improve the quality of the LEED pattern.

Experimental LEED intensity-energy [$I(E)$] curves were acquired using the video-LEED technique. The output of a charge-coupled-device camera was recorded onto video tape as the incident beam energy was ramped from 40 to 320 eV, at a rate of ~ 1 eV s⁻¹. The curves were extracted from the recording by digitizing the video image with a computer-interfaced video processor, integrating the spot intensities, and subtracting the local background around each spot. Normalization of the curves to constant incident beam current was carried out afterward. The sample was maintained at 245 K during the experiment, and was oriented for normal incidence by comparison of symmetry-equivalent curves. The time of exposure to the incident electron beam was minimized as this was found to degrade the LEED pattern. Equivalent beam averaging, a procedure known to reduce the influence of residual experimental errors,¹² was conducted whenever possible. The final data set included the (1,0), (0,1), (1,1), (2,0), (0,2), (2,1), and (1,2) curves. For reasons related to computational efficiency and accuracy, the curves were truncated to some extent on the high-energy side. The (2,2) and (3,0) curves were also measured, but were excluded from the analysis on the basis of an unacceptable signal-to-noise ratio.

III. COMPUTATIONAL PROCEDURES

Theoretical $I(E)$ curves were calculated from 30 to 260 eV, for normal incidence, with the conventional LEED package of Van Hove and Tong.¹³ After calculating reflection and transmission matrices within the self-consistent formalism, interlayer scattering was accomplished by layer doubling. Up to 43 symmetry-nonequivalent beams were included in the plane-wave expansion of the wave field, which resulted in fully converged spectra for interlayer spacings down to slightly below 1 Å. The possibility of random vacancy disorder in the S overlayer was investigated within the framework of the average t -matrix approximation (ATA).¹⁴ This method is known to be computationally valid for LEED energies on the basis of comparison to dynamical LEED calculations using the more accurate, but also more computationally demanding, coherent potential approximation (CPA).¹⁵ The fit between theoretical and experimental curves was determined quantitatively with the reliability factor of Pendry (R_P).¹⁶ Because of the extreme sen-

sitivity of this R factor to spectral noise,¹⁶ both sets of curves were smoothed twice with a three-point smoothing algorithm¹⁷ prior to the R -factor analysis.

Eight partial-wave phase shifts ($l_{\max} = 7$) were included in the calculations. In the case of S, we utilized the phase shifts of Demuth, Jepsen, and Marcus.¹⁸ As for In and P, we employed the phase shifts of Wu, Puga, and Tong.¹⁹ The phase shifts were corrected for thermal effects by allowing the S atoms to vibrate with a different amplitude than the substrate atoms, whereas In and P were assumed to have equal vibrational amplitudes. Within this framework, the optimum root-mean-square vibrational amplitude ($\langle u^2 \rangle^{1/2}$) at 245 K was determined to be 0.107 Å for S, and 0.062 Å for In and P. The R -factor value varied significantly with the treatment of thermal vibrations, but only a slight dependence was observed with regard to the final structure (changes in the optimum interlayer spacings spanned a range of less than 0.02 Å over a wide range of vibrational amplitudes). The real part of the optical potential (V_{or}) was assumed to be independent of energy, and was initially set at -10 eV. During the course of the R -factor analysis, this parameter was allowed to shift rigidly in 1-eV steps in order to obtain the best level of agreement. In the case of the optimum geometry, V_{or} was determined to be -7 eV. The imaginary part of the optical potential (V_{oi}) also was assumed to be independent of energy, and optimization of this quantity resulted in a final value of -4.2 eV.

In Fig. 1, we show a schematic representation of the (1×1) surface of InP(100). Symmetry elements of this surface include a square surface unit cell, but only a two-fold rotational axis and two orthogonal mirror planes due to the $ABCD$ stacking sequence along [100] of the zincblende lattice. One consequence of this stacking arrangement is an ambiguity of 90° in the azimuthal orientation of the crystal. In order to resolve this uncertainty, we conducted the R -factor analysis for both possible orientations. In the case of the optimum geometry, we report beam indices such that [01] in reciprocal space corresponds to [011] in real space. Note that the presence of steps does not introduce additional rotational domains,

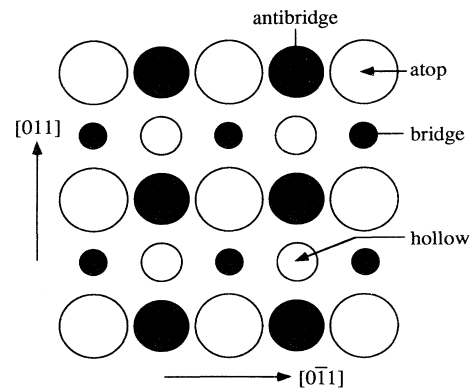


FIG. 1. Schematic of the In-terminated InP(100)-(1×1) surface showing potential high-symmetry adsorption sites for S. Light atoms correspond to In and dark atoms correspond to P. Atoms are drawn increasingly larger toward the surface.

since they must be two layers high in order to preserve the proper chemical ordering on all terraces.

The bulk lattice parameters of the epilayer were chosen to be the same as those of bulk InP(100), i.e., the bulk interlayer spacing was taken to be $d_{\text{bulk}} = 1.468 \text{ \AA}$ and the dimensions of the surface unit cell were taken to be $|a_1| = |a_2| = 4.152 \text{ \AA}$. Attempts to distort the bulk portion of the epilayer away from these values, while conserving either the bond lengths or the bond angles, always resulted in a degraded R -factor value.

IV. RESULTS AND DISCUSSION

The analysis was carried out in two stages. Initially, we sought to identify the proper binding site for the S adatoms. The high-symmetry sites that we tested include the bridge site, the atop site, the antibridge site, and the hollow site, which are shown schematically in Fig. 1. In all cases, we assumed that the substrate was terminated by a plane of In atoms, as only S-In bonds were detected by XPS in similar solution-based passivation studies.^{3,5,8,9} After determining in the proper binding site, we then optimized all structural and nonstructural parameters as well as the S coverage. Since previous studies indicated a coverage of approximately a full monolayer,^{3,8} we initially assumed that the density of atoms in the S overlayer equaled the density of atoms in each substrate layer.

For each adsorption-site model, we allowed the overlayer-substrate interlayer spacing (d_{01}) and the top-most substrate interlayer spacing (d_{12}) to vary in an independent manner. The former parameter was incremented in steps of 0.05 \AA , and the latter parameter was incremented in steps of 0.1 \AA . Since the different adsorption sites imply quite different values for d_{01} , we conducted our structural search in a manner that was appropriate for the model under consideration. More specifically, d_{01} was allowed to span the range of $1.1\text{--}2.0 \text{ \AA}$ for both the bridge-site model and the antibridge-site model, $2.0\text{--}2.8 \text{ \AA}$ for the atop-site model, and $1.0\text{--}1.6 \text{ \AA}$ for the hollow-site model. In the case of the atop-site model, the lower limit was chosen to yield a S-In bond length considerably smaller than the sum of covalent radii in order to account for the formation of a double bond. As for the possible relaxation of the substrate, d_{12} was allowed to span the range of $1.168\text{--}1.768 \text{ \AA}$.

Figure 2 compares selected best-fit theoretical $I(E)$ curves for the various adsorption-site models to those obtained experimentally. Visual inspection of the curves shows that the bridge-site model clearly yields the best level of agreement. The R -factor results also support this conclusion. After the initial crude search, the minimum R -factor values were found to be $R_p = 0.40$ for the bridge-site model, 0.73 for the atop-site model, 0.76 for the antibridge-site model, and 0.81 for the hollow-site model. The R -factor value for the bridge-site model is sufficiently lower than those for the other models to exclude the remaining models from further consideration. However, in the case of the hollow-site model there is sufficient room for the S atoms to sink lower into the substrate than allowed here. An investigation of this possibility would entail treating the S overlayer and the In plane

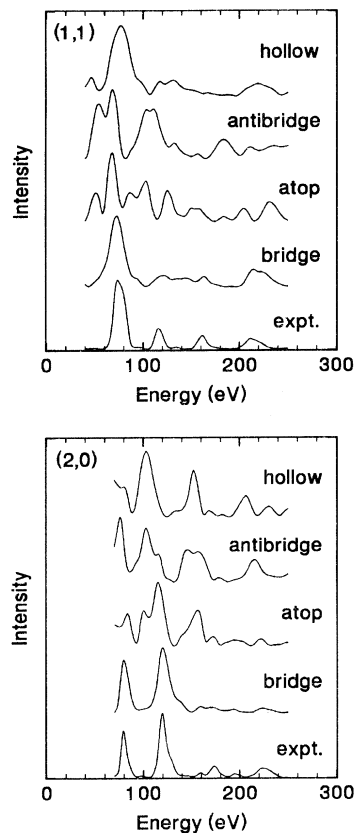


FIG. 2. Comparison between selected best-fit theoretical $I(E)$ curves for the various adsorption-site models (after the initial crude search) and those obtained experimentally.

directly beneath as a composite layer. At the present time, we do not believe that this computationally intensive step is warranted as the R -factor value remained high and practically invariant over the entire range of d_{01} that we considered. This indicates that there is no evidence for the well-known phenomenon of multiple coincidences,¹⁷ which suggests that the hollow site is not a viable adsorption site for the S atoms. Furthermore, adsorption at the hollow site is highly unlikely due to the directional bonding character of the substrate.

Since the R -factor value for the bridge-site model still left room for improvement, we refined the structure further by independently varying d_{01} and d_{12} on a 0.02-\AA grid in the vicinity of the best-fit geometry of the first stage of the analysis. In addition, we allowed the S coverage to decrease in steps of 0.1 monolayer in the lattice-gas sense in order to investigate the possibility of vacancy disorder. Furthermore, we repeatedly reoptimized the nonstructural parameters during the refinement procedure to avoid being misled by correlations with other parameters. Figure 3 compares theoretical $I(E)$ curves for the optimum geometry to those obtained experimentally. Although some minor discrepancies still exist, visual inspection of the curves shows a good overall account of both the peak positions and the relative intensities. This assessment is confirmed by an acceptable

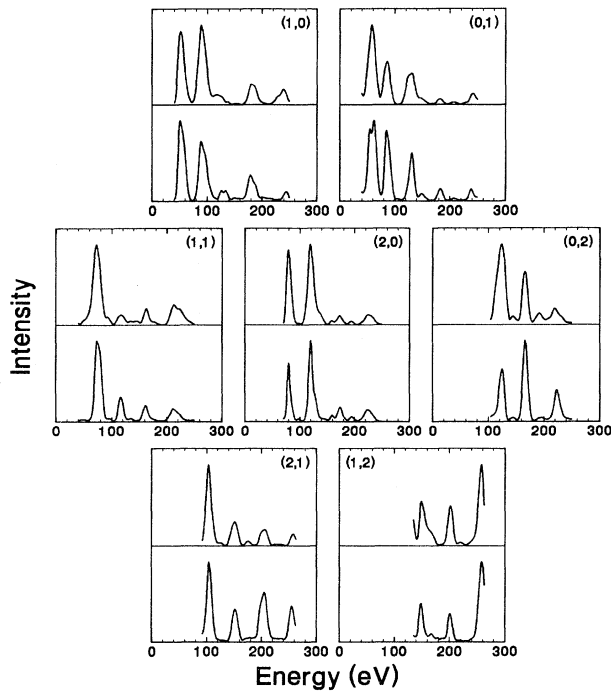


FIG. 3. Comparison between theoretical $I(E)$ curves for the optimum geometry and those obtained experimentally. The upper curves correspond to the theoretical results.

minimum R -factor value of $R_p=0.26$, which is somewhat higher than the values of less than 0.20 typically expected for simple metal surfaces, but comparable to those reported for many combinations of atomic adsorbates on metals.

Figure 4 shows plots of R_p as a function of the interlayer spacing of interest, with all other parameters fixed at their optimum values. From the position of the R -factor minimum in each plot, we deduce an optimum geometry of $d_{01}=1.445 \text{ \AA}$ and $d_{12}=1.465 \text{ \AA}$ for the S-passivated surface. In order to estimate the uncertainty

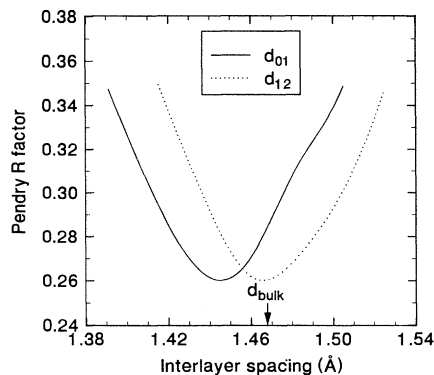


FIG. 4. Pendry R factor as a function of the interlayer spacing of interest, with all other parameters fixed at their optimum values.

in each of these quantities, we used the formula of Pendry¹⁶ to determine the standard deviation [$\Delta R = R_{\min}(8V_{oi}/\Delta E)^{1/2}$, where ΔE is the total energy range in common between experiment and theory]. Using a value of 1255 eV for ΔE , this formula yields an uncertainty of $\pm 0.033 \text{ \AA}$ for d_{01} and an uncertainty of $\pm 0.035 \text{ \AA}$ for d_{12} . Since d_{bulk} fell within the range of acceptable values for both d_{01} and d_{12} , we chose not to consider the possible relaxation of deeper interlayer spacings.

As for the S coverage, Fig. 5 shows that the R -factor results clearly favor a full monolayer as initially suggested by Tao *et al.*⁵ However, the coverage could be as low as 0.77 monolayer when the uncertainty is taken into account. Note that these values do not take into consideration the possibility of S as a substitutional impurity in the subsurface region. S is a common n -type dopant in III-V compound semiconductors, and previous studies have suggested a small concentration of S in at least the third atomic layer.^{8,9} In principle, the effect of subsurface S on the $I(E)$ curves could be modeled using the ATA method. But in this case an investigation of substitutional disorder by LEED would be unreliable due to the fact that the phase shifts of S and P are very similar, as they differ by only 1 in atomic number.

A value of $d_{01}=1.445 \text{ \AA}$ for a S atom residing in the bridge site (which can be viewed as a continuation of the zinc-blende lattice) corresponds to an In-Si-In bond angle of 110.3° . This value is very close to the tetrahedral bond angle of 109.6° , which suggests that bond formation involves the interaction of sp^3 -hybridized orbitals on both S and In, and that the bonds are predominantly covalent in nature. As a further indication of covalent bonding, the S-In bond length found here (2.529 \AA) is comparable to the bulk In-P bond length (2.543 \AA). This would be expected in the covalent limit, since the covalent radii of S and P differ by only 0.02 \AA .²⁰

The formation of two covalent S-In bonds per In atom, as implied by the bridge adsorption site, would saturate the dangling bonds on In. Experimental evidence for a bulklike environment around the In atoms in the topmost substrate plane comes from the fact that d_{12} is essentially unrelaxed. As for the remaining electrons on S, they would occupy the two sp^3 -hybridized orbitals directed

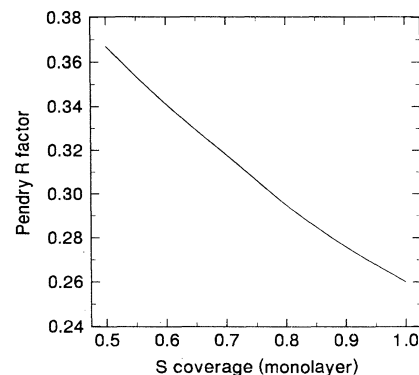


FIG. 5. Pendry R factor as a function of the S coverage, with all other parameters fixed at their optimum values.

away from the surface. A first-principles calculation by Ohno²¹ for a monolayer of S atoms on Ga-terminated GaAs(100) shows that this bonding configuration leads to a remarkably low density of states in the midgap region. Therefore the role of S in passivating the surface can be explained by the formation of covalent bridge bonds in conjunction with a low density of vacancy defects.

The results of our study confirm the model of Tao *et al.*,⁵ and are in general agreement with the previously mentioned XPD and XANES results. However, the details of the structure differ significantly. In the case of the XPD study,⁷ only a broad range of possible In-S-In bond angles has been reported so a quantitative comparison is not justified, although the largest value from that investigation is equal to the bond angle determined here. As for the XANES study,⁶ an estimated In-S-In bond angle of 100° implies a value of 1.742 Å for d_{01} , which is inconsistent with our result even when the uncertainty in d_{01} is taken into account. The recent first-principles calculation of Jin *et al.*²² also favors a much smaller distance for d_{01} than indicated by XANES. However, the results of that calculation predict that the lowest-energy structure for the S-passivated surface should correspond to an asymmetric buckled-dimer model, with an average reduction in d_{01} by 0.37 Å, an average lateral displacement of 0.45 Å off the bridge site along $[0\bar{1}1]$, and a

reduction in d_{12} by 0.07 Å. In order to explain the absence of double periodicity in the experimental LEED pattern, Jin *et al.* have suggested a random distribution of S dimers. It is not clear, though, whether this suggestion is valid as only the total energy of the perfectly ordered surface has been calculated. Moreover, we would have expected our analysis to have favored a much smaller value for d_{01} than determined here if randomly distributed dimers had been present, even with the S atoms held fixed at the bridge position. This is due to the fact that $I(E)$ curves calculated for normal incidence are rather insensitive to small lateral displacements, since momentum transfer is primarily towards the surface normal.¹⁷

ACKNOWLEDGMENTS

The support of the Natural Sciences and Engineering Research Council of Canada (NSERCC) is gratefully acknowledged. M. C. Hanf acknowledges, with thanks, the receipt of financial support from NSERCC. We also thank M. A. Van Hove for supplying the phase shifts, and Z. H. Lu for providing the InP(100) substrate, and also for sharing the results of the first-principles calculation.

¹S. Tiwari, *Compound Semiconductor Device Physics* (Academic, San Diego, 1992).

²R. Iyer, R. R. Chang, and D. L. Lile, *Appl. Phys. Lett.* **53**, 134 (1988).

³C. W. Wilmsen, K. M. Geib, J. Shin, R. Iyer, D. L. Lile, and J. J. Pouch, *J. Vac. Sci. Technol. B* **7**, 851 (1989).

⁴H. Oigawa, J. Fan, Y. Nannichi, H. Sugahara, and M. Oshima, *Jpn. J. Appl. Phys.* **30**, L322 (1991).

⁵Y. Tao, A. Yelon, E. Sacher, Z. H. Lu, and M. J. Graham, *Appl. Phys. Lett.* **60**, 2669 (1992).

⁶Z. H. Lu, M. J. Graham, X. H. Feng, and B. X. Yang, *Appl. Phys. Lett.* **60**, 2773 (1992).

⁷Z. H. Lu (unpublished).

⁸D. Gallet and G. Hollinger, *Appl. Phys. Lett.* **62**, 982 (1993).

⁹Y. Fukuda, Y. Suzuki, N. Sanada, S. Sasaki, and T. Ohsawa, *J. Appl. Phys.* **76**, 3059 (1994).

¹⁰G. W. Anderson, M. C. Hanf, P. R. Norton, Z. H. Lu, and M. J. Graham, *Appl. Phys. Lett.* **65**, 171 (1994).

¹¹G. W. Anderson, M. C. Hanf, J. G. Shapter, P. R. Norton, Z. H. Lu, and M. J. Graham, *Surf. Sci.* **318**, 299 (1994).

¹²H. L. Davis and J. R. Noonan, *Surf. Sci.* **115**, L75 (1982).

¹³M. A. Van Hove and S. Y. Tong, *Surface Crystallography by LEED* (Springer, Berlin, 1979).

¹⁴B. L. Gyorffy and G. M. Stock, in *Electronics in Disordered Metals and Metallic Surfaces*, edited by P. Phariseau, B. L. Gyorffy, and L. Scheire (Plenum, New York, 1979).

¹⁵S. Crampin and P. J. Rous, *Surf. Sci.* **244**, L137 (1991).

¹⁶J. B. Pendry, *J. Phys. C* **13**, 937 (1980).

¹⁷M. A. Van Hove, W. H. Weinberg, and C-M. Chan, *Low-Energy Electron Diffraction* (Springer, Berlin, 1986).

¹⁸J. E. Demuth, D. W. Jepsen, and P. M. Marcus, *Surf. Sci.* **45**, 733 (1974).

¹⁹X. J. Wu, M. W. Puga, and S. Y. Tong, in *Surface Physics*, edited by X. Xie (World Scientific, Singapore, 1987).

²⁰B. Douglas, D. H. McDaniel, and J. J. Alexander, *Concepts and Models of Inorganic Chemistry* (Wiley, New York, 1983).

²¹T. Ohno, *Surf. Sci.* **255**, 229 (1991).

²²J. M. Jin, M. W. C. Dharma-wardana, D. J. Lockwood, Z. H. Lu, G. C. Aers, and L. W. Lewis (private communication).